SCIENCE CHINA
Chemistry

• REVIEWS •
• SPECIAL TOPIC • Biophysical Chemistry

December 2014 Vol.57 No.12: 1634–1645
doi: 10.1007/s11426-014-5234-4

Self-assembly of surfactant-like peptides and their applications

ZHANG JingHui, ZHAO YuRong, HAN ShuYi, CHEN CuiXia & XU Hai*

Centre for Bioengineering and Biotechnology, China University of Petroleum (East China), Qingdao 266580, China

Receieved July 9, 2014; accepted August 25, 2014; published online November 5, 2014

Numerous peptides derived from naturally occurring proteins or *de novo* designed have been found to self-assemble into various nanostructures. These well-defined nanostructures have shown great potential for a variety of biomedical and biotechnological applications. In particular, surfactant-like peptides (SLPs) have distinctive advantages in their length, aggregating ability, and water solubility. In this article, we report recent advances in the mechanistic understanding of the self-assembly principles of SLPs and in their applications, most of which have been made in our laboratory. Hydrogen bonding between peptide backbones, hydrophobic interaction between hydrophobic side chains, and electrostatic repulsion between charged head groups all have roles in mediating the self-assembly of SLPs; the final self-assembled nanostructures are therefore dependent on their interplay. SLPs have shown diverse applications ranging from membrane protein stabilization and antimicrobial/anticancer agents to nanofabrication and biomineralization. Future advances in the self-assembly of SLPs will hinge on their large-scale production, the design of new functional SLPs with targeted properties, and the exploitation of new or improved applications.

surfactant-like peptides, self-assembly, mechanism, applications

1 Introduction

Enormous complex and functional biological entities are achieved through hierarchical self-assembly [1, 2]. Self-assembly of biomolecules (e.g., peptides, proteins, nucleic acids, and lipids) is the basis of the hierarchy, complexity, and functionality of living organisms. Typical biomolecular self-assembly systems include lipid bilayers and vesicles, DNA double helices, folded polypeptides and proteins (e.g., collagen triple helix and hemoglobin), and complex molecular machines (e.g., ribosomes and light-harvesting systems). These supramolecular assemblies not only have well-defined nanostructures but also perform specific functions with astonishing precision and efficiency; these features are essential to the existence and continuation of life. In addition, the relationships between the self-assembled structures and their functions are tightly constrained. For example, the failure of proteins to remain correctly folded is the origin of many human diseases [3].

Over the past two decades, advances in synthetic methodologies for nucleic acids and peptides, together with the advent of genetic engineering, have made available a wealth of biomolecular building blocks and have thereby fueled numerous studies in the area [4–12]. These studies have focused primarily on two complementary aspects: the first is to unveil the principles and rules that govern the self-assembly processes and the assembled architectures of biomolecules; the second is to fabricate functional nanostructures by mimicking biomolecular self-assembly for targeted applications in diverse fields.

Relative to large and complex polypeptides, proteins, and nucleic acids, short peptides (typically less than 30 residues) have distinctive advantages including ease of synthesis, structural stability, easier establishment of the relationship between molecular structures and self-assembly, and rational interpretation of various interactions involved in self-assembly. In spite of their short lengths, combinations of the 20 natural amino acids with numerous non-natural ones

*Corresponding author (email: xuh@upc.edu.cn)

endow them with a huge sequence diversity as well as good accessibility to chemical and biological modifications. As a consequence, the self-assembly of short peptides has received extensive attention as one of the most useful organic building blocks [12–21]. Considerable self-assembling short peptides have thus been investigated, including peptide fragments from naturally occurring polypeptides and proteins, *de novo* designed ones, and peptide derivatives with aromatic, aliphatic and/or phospholipid moieties. Table 1 lists representative self-assembling short peptides including cyclic peptides, ionic complementary peptides, peptide amphiphiles (PAs), hairpin peptides, amyloid peptide fragments and derivatives, multidomain peptides, helical peptides, and surfactant-like peptides (SLPs) [6–9, 15–18, 22–69]. Obviously, various nanostructures have been achieved through short peptide self-assembly; moreover, these self-assembled nanostructures have shown potential for a variety of biotechnological and biomedical applications including cell culture and tissue engineering, regenerative medicine, drug delivery, antibacterial biomaterials, enzyme immobilization and biosensing, biomineralization and nanofabrication, and membrane protein solubilization and stabilization. These peptides have also served as idealized models for studies of polypeptide and protein folding and misfolding, which is helpful in understanding both normal and abnormal biological functions (e.g., Alzheimer's and Parkinson's diseases).

During self-assembly, these short peptides usually undergo structural transitions from random coils to folded structures such as β-sheets, β-turns, and α-helices. These structural transitions, which indicate the formation of intra- and/or intermolecular hydrogen bonding, are also associated with the formation of amphiphilic conformations. For example, upon folding into β-sheet and α-helical structures, ionic complementary peptides, hairpin peptides, multidomain peptides, and helical peptides form facially amphiphilic conformations with hydrophobic residues on one face of the peptide and hydrophilic residues on the other. In fact, amphiphilicity plays a critical role in protein folding and peptide self-assembly by providing well-defined hydrophobic collapse and electrostatic interaction.

As two representative linear amphiphilic peptides with distinctly hydrophobic and hydrophilic ends, PAs are composed of polar peptide sequences and apolar aliphatic chains; SLPs consist exclusively of amino acid residues. For SLPs, several consecutive hydrophobic residues constitute hydro-

Table 1 Summary of self-assembling peptides [6–9, 15–18, 22–69]

Types	Typical sequences [a]	Assembled nanostructures	Applications	Ref.
Cyclic peptides	(AEAQAEAQ) (WLWLWLQL) (KQRWLWLW)	Nanotubes	Artificial transmembrane ion channels and antimicrobial agents	[6, 22, 23]
Ionic complementary peptides	Ac-(AEAEAKAK)$_2$-NH$_2$ Ac-(RADA)$_4$-NH$_2$ Ac-(KLDL)$_3$-NH$_2$ Ac-QQKFQFQFEQQ-NH$_2$ Ac-QQRFQWQFEQQ-NH$_2$	Nanofibrils and nanosheets	Cell culture and regenerative scaffolds, tissue engineering, drug delivery, and biosensing	[7, 24–28]
Peptide amphiphiles (PAs)	C$_{16}$H$_{31}$O-CCCCGGGS$^{(PO4)}$RGD C$_{16}$H$_{31}$O-AAAGGGEIKVAV C$_{16}$H$_{31}$O-VEVE C$_{16}$H$_{31}$O-VVVAAAEEE C$_{16}$H$_{31}$O-KKK-NH$_2$	Nanofibrils, nanobelts, nanotubes, and nanomicelles	Nanofabrication, biomineralization, cell culture scaffolds, tissue engineering, and antimicrobial agents	[8, 16, 29–32]
Hairpin peptides	(VK)$_4$VPPT(KV)$_4$-NH$_2$ (VK)$_4$VPPTKVEV(KV)$_2$-NH$_2$	Nanofibrils	Cell culture scaffolds, drug delivery, biomineralization	[33, 34]
Amyloid peptide fragments and derivatives	FF or FF-NH$_2$ Fmoc-FF KLVFFAE Ac-KLVFFAE-NH$_2$	Nanotubes, nanofibrils, and nanovesicles	Cell culture scaffolds, drug delivery, nanofabrication, biosensing	[9, 17, 35–37]
Multidomain peptides	Ac-K$_2$(QL)$_6$K$_2$-NH$_2$ Ac-E$_2$(SL)$_6$E$_2$GRGDS-NH$_2$	Nanofibrils	Cell culture, drug delivery, biosensing	[38, 39]
α-Helical peptides	KIAALKAKIAALKAEIAALEAENAALEA KIAALKQKIASLKQEIDALEYENDALEQ	Nanofibrils	Cell culture	[40]
Surfactant-like peptides (SLPs)	Ac-X$_6$D$_{1-2}$ (X = A, V, L) Ac-G$_m$D$_2$ (m = 4, 6, 8, 10) Ac-X$_6$K$_{1-2}$-NH$_2$ (X = A, V, L) Ac-A$_9$K-NH$_2$ Ac-I$_m$K$_n$-NH$_2$ (m = 3–4, n = 1–2) Ac-KI$_4$K-NH$_2$ Ac-AAVVLLLWEE Ac-GAVILRR-NH$_2$ Ac-IVD Ac-LIVAGD A$_6$R	Nanofibrils, nanobelts, nanotubes, nanomicelles, and nanovesicles	Biomineralization, antibacterial agents, and membrane protein stabilization	[15, 18, 41–69]

a) Single-letter codes for amino acids. The brackets indicate cyclic peptide structure and underlining represents D-amino acids.

phobic tails and one or two hydrophilic charge residues serve as heads. Stupp's research group [8, 16, 29–31] has contributed significantly to PA design, self-assembly, and related applications. The Zhang group [41–45] pioneered SLP self-assembly and applications in membrane protein stabilization. In contrast to conventional surfactants, the advantages of linear amphiphilic peptides are that biologically active sequences (e.g., RGD) can be incorporated into their molecular structures and there is hydrogen bonding between their backbones. In comparison with other self-assembling peptides, the specific advantages of SLPs lie in their short length (typically less than 10 residues) and high solubility in aqueous solutions (Table 1). As examples, ultrashort SLPs containing three or four residues such as Ac-IVD and Ac-IIIK-NH_2 have been found to readily self-assemble into long fibers in water [46, 47]; A_6K shows high solubility in water up to ~12 wt% and forms a nematic phase consisting of long assembled nanotubes at ~17 wt% [48]. Although some short FF-containing peptides (e.g., FF and KLVFFAE) can also form long tubes or fibers, they show poor water solubility and their self-assembly in aqueous solutions is usually realized by adding organic solvents such as 1,1,1,3,3,3-hexafluoro-2-propanol or acetonitrile [9, 35–37, 70]. As shown in Table 1, the range of self-assembling peptide building blocks is so wide that it would be impossible to cover the entire spectrum in a single article. Here, we focus on the self-assembly principles of SLPs and their applications, with particular emphasis on results from our own laboratory.

2 Principles of SLP self-assembly

2.1 Critical aggregation concentration (CAC)

Just like conventional surfactants, most SLPs have well-defined CACs (Table 2) and some of the general rules for conventional surfactants are also applicable to SLPs. For example, increasing molecular hydrophobicity via the number of hydrophobic amino acid residues (e.g., Ac-I_mK-NH_2 and Ac-L_mK-NH_2, m = 3–5) or the size of hydrophobic side chains (e.g., Ac-G_6K-NH_2, Ac-A_6K-NH_2, and Ac-V_6K-NH_2; as well as Ac-A_6D and Ac-V_6D) obviously lowers their CACs [50, 53–55]. Similarly, the use of PBS buffer results in a reduction in the CAC values due to the decreased electrostatic repulsion between ionic head groups as well as the decreased hydration of hydrophobic moieties [49, 52]. Note that different CAC values have been obtained for the same SLP. The values derived from the conductivity method appear to be lower than those from DLS and fluorescence methods, for example, 0.2, 0.5, and 1.05 mmol/L for Ac-A_6K-NH_2, respectively [49, 53, 55]. Each of these methods responds to a different feature of the aggregation, which may be more distinct than for conventional surfactants.

Because most studies on SLP self-assembly and applications (e.g., the stabilization of membrane proteins) are performed above the CAC and the CAC values can work as a useful indication of their structural propensity for self-assembly, it is essential to know the CAC values of SLPs. For example, we have found that Ac-I_3K-NH_2 has a markedly lower CAC value in water than Ac-L_3K-NH_2 does, in spite of their similar hydrophobicity [54]. This difference is ascribed to the stronger β-sheet forming propensity of isoleucine, which leads to β-sheet structuring during the self-assembly of Ac-I_3K-NH_2 molecules and thus promotes their aggregation. In contrast, unordered structure dominates during the Ac-L_3K-NH_2 self-assembly. With an increase in the number of hydrophobic residues, Ac-I_5K-NH_2 and Ac-L_5K-NH_2 have converged to nearly identical CACs at a lower value (Table 2) [47, 49–55]. The increase in hydrophobicity evidently induces the formation of β-sheet hydrogen bonding in the case of Ac-L_5K-NH_2 [54].

2.2 The roles of noncovalent forces and their cooperativity

Molecular self-assembly is driven by various noncovalent interactions among numerous building blocks. Although each of these interactions is rather weak, their collective action can result in very stable structures and materials [10]. As for SLPs, hydrogen bonding, hydrophobic, and electrostatic interactions are widely regarded as the main forces

Table 2 CACs of SLPs and determination methods [47, 49–55]

Sequences	Media	CACs (mmol/L)	Methods	Ref.
Ac-A_6K-NH_2 Ac-A_6D	Water/PBS	1.02/0.14 0.46/0.3	Dynamic light scattering (DLS)	[49]
Ac-V_6D, Ac-A_6D, Ac-V_6D_2	Water	0.5, 1.6, 1.1	DPH fluorescence	[50]
Ac-AAVVLLLWEE	PBS	0.49	Tryptophan fluorescence	[51]
Ac-GAVILRR-NH_2	Water/PBS	0.82/0.45	DLS	[52]
Ac-A_6K-NH_2, Ac-A_9K-NH_2	Water	0.2, 0.017	Electric conductivity	[53]
Ac-I_3K-NH_2	Water	0.43	Pyrene fluorescence	[47]
Ac-I_3K-NH_2, Ac-I_4K-NH_2, and Ac-I_5K-NH_2	Water	0.41/0.25/0.13	Electric conductivity	[54]
Ac-L_3K-NH_2, Ac-L_4K-NH_2, and Ac-L_5K-NH_2	Water	1.15/0.54/0.14	Electric conductivity	[54]
Ac-G_6K-NH_2, Ac-A_6K-NH_2, and Ac-V_6K-NH_2	Water	–/0.5/0.15	Pyrene fluorescence	[55]

that drive their self-assembly, and each type of interaction plays a distinctive role in mediating the self-assembly processes.

Hydrogen bonding

Unlike conventional surfactants that typically self-assemble into micelles and vesicles [71], most SLPs readily self-assemble into high-aspect-ratio nanostructures (e.g., nanofibrils, nanoribbons, and nanotubes) and adopt β-sheet secondary structures. To establish the relationship between β-sheet hydrogen bonding and self-assembled architectures, we designed and synthesized two series of peptides, Ac-I_mK-NH_2 and Ac-L_mK-NH_2 (m = 3–5) [54]. I and L are isomeric amino acids with four-carbon side-chains; the former is well known to have a stronger propensity than the latter for β-sheet forming [72]. Circular dichroism (CD) and FTIR characterizations show that Ac-I_mK-NH_2 molecules predominantly adopt β-sheet structures upon self-assembly in water (pH 6.0), whereas Ac-L_3K-NH_2 adopts random coil conformation [47, 54]. TEM characterization and thioflavin-T (ThT) binding assays indicate that the Ac-I_mK-NH_2 peptides self-assemble into long nanofibrils that are structurally similar to amyloid fibrils in that both adopt cross-β structures in which the alignment of the peptide backbones (β-strands) is approximately perpendicular to the fibril axis and the hydrogen bonding between strands is approximately parallel to the fibril axis. In contrast, Ac-L_3K-NH_2 forms spherical stacks due to the lack of β-sheet structuring (Figure 1). However, an increase in the number of leucines induces the formation of β-sheet structuring in Ac-L_5K-NH_2, possibly due to the cooperative effect of hydrophobic interaction and hydrogen bonding. As a result, the extension of hydrogen bonding leads to the formation of long Ac-L_5K-NH_2 nanofibrils (Figure 1). As expected, the self-assembly of Ac-LI_2K-NH_2 and Ac-L_4K-NH_2 is intermediate between Ac-I_3K-NH_2 or Ac-L_5K-NH_2 and Ac-L_3K-NH_2; that is, they form short fibrils and spherical stacks in which β-sheet and unordered secondary structures coexist [54].

Baumann *et al.* [56] performed a similar study with Ac-X_6K_2-NH_2 (X = I, V, L) peptides. Here, the Ac-I_6K_2-NH_2 self-assembles into flat ribbonlike structures in 2 mmol/L NaCl aqueous solution and Ac-L_6K_2-NH_2 and Ac-V_6K_2-NH_2 form short rodlike fibrils and globular aggregates. The CD characterization indicates that the former adopts β-sheet conformations and the latter two predominantly adopt random coil structures. A recent review claimed that these findings are unusual because even short fibrils are usually associated with ordered secondary structures (usually β-sheet) [18]. In fact, the problem may lie with the CD characterization, which usually cannot provide detailed structural information when the spectrum is an average of different CD signals derived from various secondary structures with distinctly different intensities. One way of addressing this issue is with a combination of CD and FTIR. Our study has demonstrated that although the CD spectrum of Ac-L_4K-NH_2 is only indicative of the formation of unordered structures, the complementary FTIR characterization shows the marked occurrence of a shoulder peak at 1621 cm^{-1}, which is characteristic of β-sheets, in addition to the main peak at 1648 cm^{-1}. These peaks suggest the coexistence of dominant unordered and limited β-sheet structures [54]. Therefore, it is most likely that the formation of short fibrils in the cases of Ac-L_4K-NH_2, Ac-L_6K_2-NH_2, and Ac-V_6K_2-NH_2 is also caused by the extension of hydrogen bonding networks and the spherical aggregates correspond to unordered secondary structures.

Hauser *et al.* [19, 46, 57] have recently designed and synthesized specific SLPs of 3–6 residues (e.g., Ac-LIVAGD, Ac-LIVAD, and Ac-IVD). For these SLPs, the hydrophobic amino acids in the N-terminal hydrophobic tail decrease in size toward the C-terminal hydrophilic region. This decrease leads to unique conformational changes during their self-assembly, from random coil to α-helical intermediates terminating in cross-β peptide structures (Figure 2). As expected, these peptides eventually form amyloid-like fibrils. These findings are unusual because it is generally assumed that short linear peptides of less than 7 residues cannot form α-helical structures in aqueous solutions as there are insufficient amino acids for the formation of a complete turn of the helix.

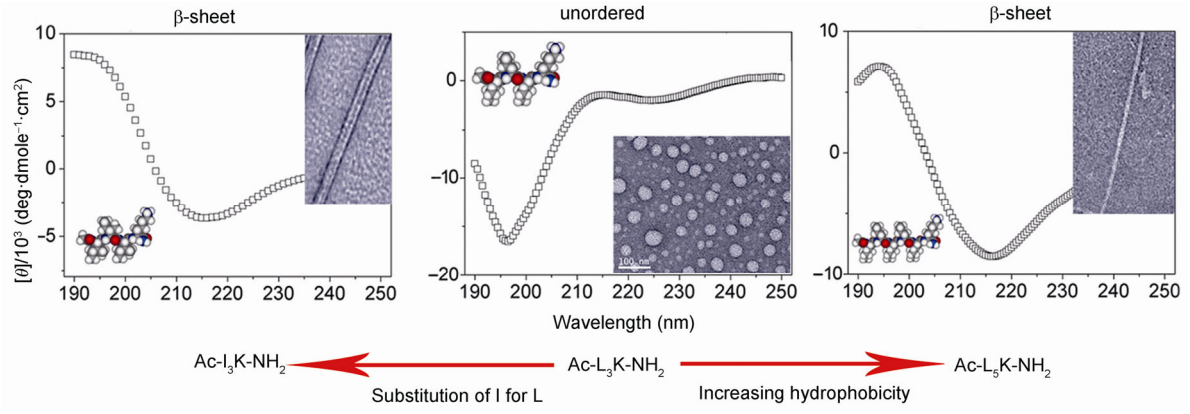

Figure 1 The role of hydrogen bonding and its cooperativity with hydrophobic interaction during the self-assembly of short SLPs [54].

Hydrophobic interaction

In water, hydrophobic interaction promotes aggregation of hydrophobic units. SLPs have distinct hydrophobic and hydrophilic segments. Hydrophobic forces drive the nonpolar region of each SLP toward one another, away from the water, thus minimizing their exposure to water [10]. Just as for conventional surfactants, increasing the hydrophobicity of SLPs favors aggregation, which is manifested by the variations of the CAC with the number and hydrophobicity of hydrophobic amino acids (Table 2). As the primary thermodynamic driving force for assembly in water, hydrophobic interaction provides limited control over shape and structure compared with hydrogen bonding [38]. However, for β-sheet forming SLPs, the self-assembled geometries do show some dependence on their hydrophobicity. In the case of Ac-A_mK-NH_2 (m = 3, 6, 9), the three peptides all adopt predominantly β-sheet structures but form different morphologies: stacked bilayers (Ac-A_3K-NH_2), long cylindrical nanofibrils (Ac-A_6K-NH_2), and short nanorods and micelles (Ac-A_9K-NH_2) (Figure 3) [58]. Ac-I_mK-NH_2 (m = 3, 4, 5) all form nanofibrils with predominantly β-sheet structures but their diameters decrease with an increase in the number of hydrophobic residues [54]. The dimensional reduction can be interpreted using the molecular packing theory developed to describe surfactant structural transitions. With increasing hydrophobic tail length, the entropic gain, decreased CACs, and increased electrostatic repulsion between the head groups lead to a lowering of the packing parameter (p) [58]. It is widely accepted that spherical micelles form with $0 \leqslant p \leqslant 1/3$, cylindrical micelles form with $1/3 \leqslant p \leqslant 1/2$, and bilayer or lamellar sheets form with $1/2 \leqslant p \leqslant 1$ [73]. Compared to Ac-A_6K-NH_2, Ac-V_6K-NH_2 has been observed to form bilayer sheets [55]. This observation seems to contradict the above trend with increasing hydrophobicity for SLPs. However, detailed AFM characterization reveals that these bilayer stacks form through a morphological transition from thinner nanofibrils, possibly driven by the structural symmetry of the valine side chain.

Electrostatic interaction

SLPs contain charged residues as their hydrophilic heads. Upon self-assembly in aqueous solutions, the charged residues

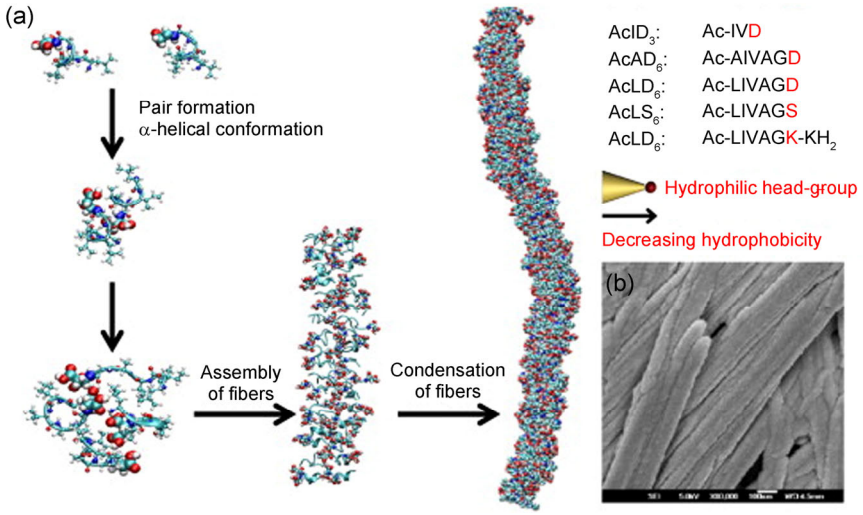

Figure 2 (a) Suggested scheme for self-assembly from peptide monomers to supramolecular networks of condensed fibers. Self-assembly is initiated with antiparallel pairing of two peptide monomers by changing to a α-helical conformation. Subsequently, peptide pairs assemble to fibers and nanostructures and condense to fibrils, resulting in hydrogel formation. (b) FESEM image of fibers formed from Ac-LIVAGD peptide [19].

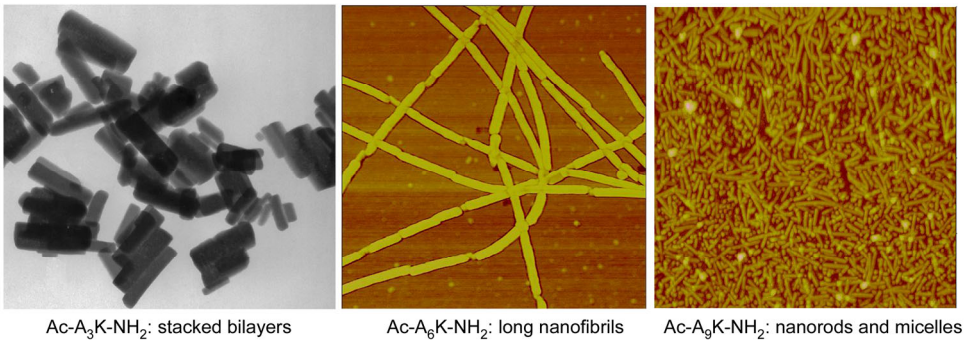

Figure 3 Different self-assembled nanostructures by Ac-A_3K-NH_2 (stacked bilayers), Ac-A_6K-NH_2 (long cylindrical nanofibrils), and Ac-A_9K-NH_2 (short nanorods and micelles) [58].

are oriented toward the surface to facilitate hydration and solubility of the assemblies. The electrostatic interaction between these adjacent charged groups then has a profound influence on the self-assembled architectures. Electrostatic interaction can be either attractive or repulsive, depending on the signs of the charges. For most of the reported SLPs, the polar regions usually consist exclusively of similarly charged residues and the terminal opposite charges are usually eliminated by terminal capping during synthesis (acetylation or amidation). Thus, it is electrostatic repulsion that plays the important role. We note that electrostatic attraction will dominate mixtures of cationic/anionic SLPs and that such mixing then leads to dramatic decreases in CACs and more complicated self-assembly behaviors [59]. Here we focus on the self-assembly of individual SLPs rather the mixing of different SLPs, and discuss only electrostatic repulsion in detail.

Unlike hydrogen bonding and hydrophobic interactions that promote the aggregation of SLPs and the axial growth of their self-assembly (anisotropy), electrostatic repulsion favors curvature of self-assembled architectures. We have systematically investigated the role of electrostatic interaction through terminal capping of short Aβ (16–22) peptides [37]. For KLVFFAE and Ac-KLVFFAE-NH_2, charged groups appear largely on their N-terminal ends at pH 2.0, which make them surfactant-like. In both cases, hydrogen bonding between β-strands occurs along the axial direction, whereas the hydrophobic interaction and aromatic stacking of side chains between β-sheets occur along the lateral direction (Figure 4). In the case of KLVFFAE, each molecule carries two positive charges at its N-terminus; the strong electrostatic repulsion between the charged head groups of KLVFFAE molecules disfavors lateral stacking of β-sheets and instead favors interfacial twisting and curving of β-sheets, which eventually leads to the formation of cylindrical fibrils with diameters of ~3.8 nm. In contrast, each Ac-KLVFFAE-NH_2 carries one positive charge and the intermolecular electrostatic repulsion is dramatically reduced. As a result, a stronger lateral stacking of β-sheets occurs that eventually results in the formation of bilayer tapes with widths of ~70 nm.

Variation of pH and addition of salts may change the electrostatic repulsion through the protonation or deprotonation of the basic/acidic residues and the screening of their charges. The self-assembled morphologies of SLPs can therefore be easily modulated by tuning the pH and ionic strength of the solution. In a study on the effect of salts on the self-assembly of cationic SLPs (Ac-A_9K-NH_2 and Ac-I_3K-NH_2), we found that anions have more pronounced effects than cations in tuning the self-assembled nanostructures [74]. Addition of ClO_3^-, NO_3^-, and Br^- can stabilize the primary assembled nanostructures (nanostacks, nanospheres, or short nanorods) and effectively inhibit their growth into longer nanostructures (nanorods or nanotubes). In contrast, the anions of Cl^-, SO_4^{2-}, HPO_4^{2-}, PO_4^{3-}, and $C_6H_5O_7^{3-}$ (citrate) favor the axial growth of these peptides to form long intersecting nanofibrils and lead to increased diameter and surface roughness as well, both of which clearly enhance their propensity for nanostructuring. The efficiency of different anions in promoting the growth of peptide nanoaggregates into larger ones can be ordered as $ClO_3^- < NO_3^- \leqslant Br^- < Cl^- < SO_4^{2-} < HPO_4^{2-} < PO_4^{3-} < C_6H_5O_7^{3-}$, which is broadly consistent with the Hofmeister anion sequence.

Cooperativity

Hydrogen bonding, hydrophobic interaction, and electrostatic repulsion are the main driving forces for SLP self-assembly. Intermolecular β-sheet hydrogen bonding drives the axial growth of peptide assembly by aligning β-strands, hydrophobic interaction promotes aggregation by shielding hydrophobic moieties from the aqueous environment, electrostatic repulsion favors the curvature formation of the assembled architectures.

The final self-assembled nanostructures are dependent on the delicate balance of these noncovalent forces. As indicated

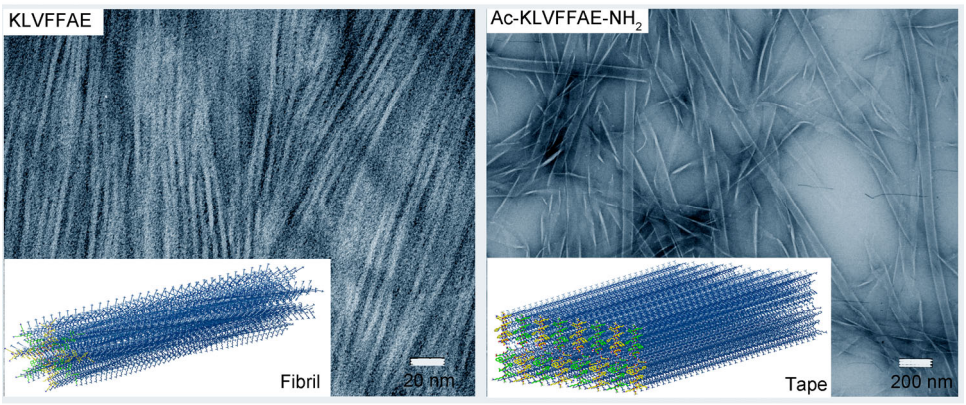

Figure 4 Different self-assembled nanostructures formed by KLVFFAE and Ac-KLVFFAE-NH_2 at pH 2.0 [37].

above, the self-assembly of Ac-L_5K-NH_2 is indicative of the cooperative effect of hydrophobic interaction and hydrogen bonding, that is, raising hydrophobicity by increasing the number of leucine residues induces β-sheet hydrogen bonding and results in the formation of ordered aggregates [54]. In a recent study, we have more systematically shown the cooperative effect of the above forces on the self-assembled nanostructures by using three specially designed peptides: Ac-I_4K_2-NH_2, Ac-KI_4K-NH_2, and Ac-$I_2K_2I_2$-NH_2 [60]. These three peptides have the same amino acid composition but different sequences. Ac-I_4K_2-NH_2 and Ac-KI_4K-NH_2 self-assemble into long nanofibrils and nanotubes, respectively, with predominantly β-sheet structures. This structural difference arises from the interplay of hydrophobic contact and electrostatic repulsion. For Ac-I_4K_2-NH_2, the electrostatic repulsion acts on the asymmetric molecular geometry and weakens the hydrophobic attraction between β-sheets, thus leading to limited stacking and significant twisting and eventually giving rise to fibrillar morphology (Figure 5(a)). In the symmetric molecular geometry of Ac-KI_4K-NH_2, the hydrophobic attraction is much less influenced by the electrostatic repulsion, which results in the formation of the wide ribbons that slowly develop into nanotubes (Figure 5(b)). Due to the lack of the alignment induced by the β-sheet hydrogen bonding, no well-defined self-assembled structure forms from Ac-$I_2K_2I_2$-NH_2.

3 Applications

3.1 Stabilization of membrane proteins

Membrane proteins not only play essential roles in various vital cellular activities (e.g., energy conversion, photosynthetic electron transport, cell signaling, cell-cell interactions, cell adhesion, and cell migration and movement) but also act as natural biosensors for hearing, smell, taste, touch, and sight in living organisms [75–78]. They are therefore of great importance in current structural biology and bionanotechnology. Away from the natural lipid bilayer environment, however, membrane proteins easily aggregate, which

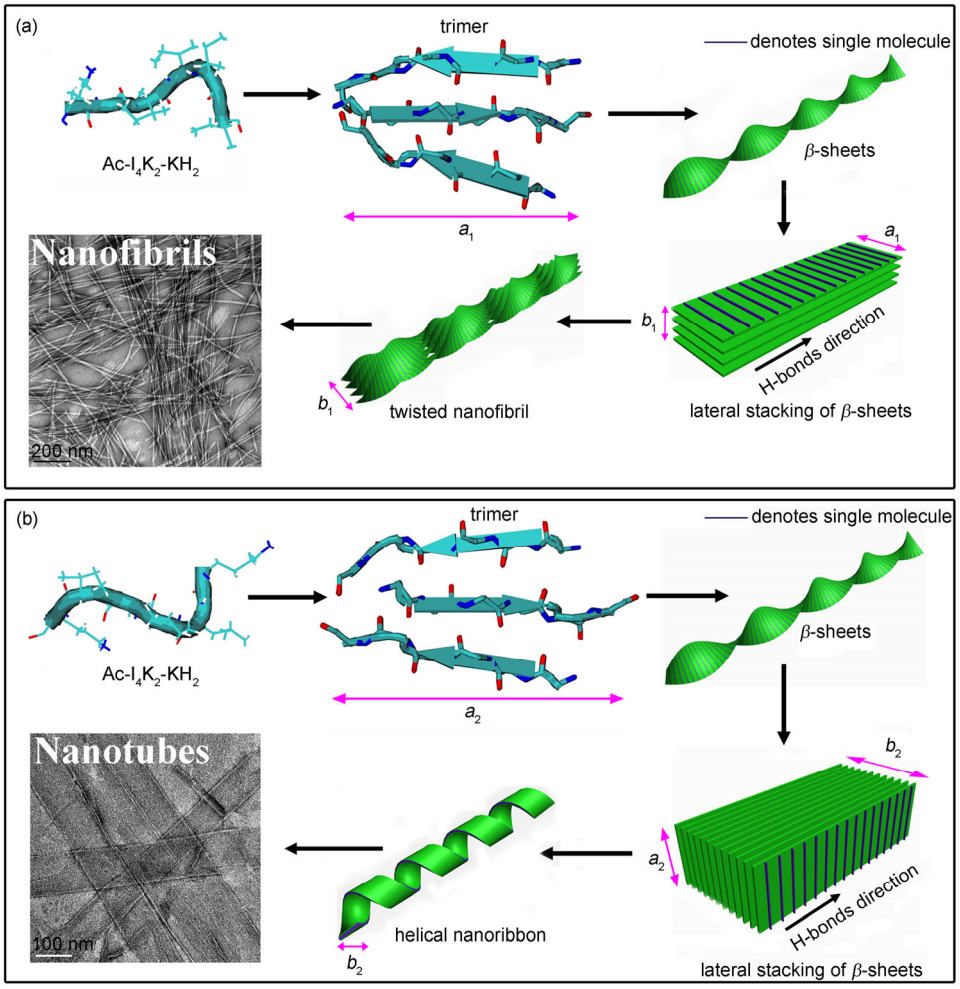

Figure 5 Schematic representation of the hierarchical self-assembly processes of Ac-I_4K_2-NH_2 (a) and Ac-KI_4K-NH_2 (b), which consist of three main steps: the formation of β-sheets, lateral stacking of β-sheets, and the evolution of stacked β-sheets into nanofibrils or nanotubes due to inherently twisting of β-sheets. a_1 and a_2: the thicknesses of β-sheets, which are equal to those of the lamellae arising from their stacking; b_1 and b_2: lamination of β-sheets [60].

leads to significant losses of structure and function. The solubility and stability of membrane proteins have thus not only significantly impeded structural and functional studies but have also limited their applications. Current structural studies are mostly accomplished by using synthetic or natural chemical surfactants, but these surfactants do not always favor the long-term stability of the proteins; in addition, some surfactants with high solubilizing ability often have denaturing properties. It is therefore highly desirable to find alternative surfactants to solubilize and stabilize membrane proteins with well-retained structures and functions.

Because SLPs are compositionally identical to proteins and structurally similar to conventional surfactants, they have shown great potential for stabilizing membrane proteins [44, 45, 61, 75]. Using Ac-V_6D, Ac-A_6D, and Ac-A_6K-NH_2, Zhang and co-workers [75] reported the stabilization of a G-protein-coupled receptor (GPCR) bovine rhodopsin in aqueous solution. These SLPs give a better stabilizing effect than the commonly used membrane-protein-stabilizing surfactants such as *n*-dodecyl-D-maltoside (DM) and *n*-octyl-D-glucoside (OG). Ac-A_6D can not only synergistically interact with the surfactants OG and DM and lipids to enhance rhodopsin stability but also can effectively protect rhodopsin function against thermal denaturation in the absence of both lipid and conventional surfactants. A proposed model for the rhodopsin stabilization by Ac-A_6D is shown in Figure 6. We have designed a series of SLPs to increase the thermal stability of a multi-domain protein complex photosystem-I (PS-I) [61]. Of all the short peptides we studied, Ac-I_5K_2-NH_2 shows the best stabilizing effect by enhancing the melting temperature of PS-I from 48.0 to 53.0 °C at a concentration of 0.65 mmol/L and by significantly extending the half-life of isolated PS-I.

However, the principles of how SLPs stabilize membrane proteins are not well understood. This understanding is the primary goal of future research in which an essential step

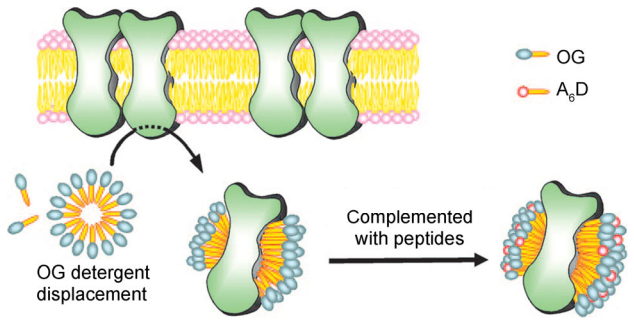

Figure 6 A proposed model of GPCR bovine rhodopsin stabilization using peptide surfactants. GPCR bovine rhodopsin was extracted with OG (gray heads) from the lipid membrane (pink heads). After surfactant exchanges, the hydrophobic alanine tail of Ac-A_6D (red heads) forms the rhodopsin-surfactant complex only on the belt area. Small peptide surfactants surround the rhodopsin and act to protect it from thermal denaturation in a way that is similar to the action of chaperones. This action may be similar to that of lipids and other surfactants as well. Note that all hydrophobic tails are shown in yellow [75].

will be the rational design and use of SLPs to stabilize certain membrane proteins for prolonged periods, as well as for structural and functional studies and applications.

3.2 Templates for nanofabrication and biomineralization

Charge residues and their combinations with other residues often possess biological and chemical functions (e.g., RGD or RGDS). As the head group of SLPs, these polar residues are mostly distributed on the surface of their self-assemblies in the aqueous environment, thus making the self-assembled nanostructures particularly active for creating novel nanodevices.

The long nanotubes formed by Ac-I_3K-NH_2 self-assembly show exceptionally high structural stability and morphological integrity in extreme conditions [47]. The Ac-I_3K-NH_2 nanotubes have been used as soft templates for the templating of the sol-gel condensation of tetraethoxysilane (TEOS) at neutral pH, yielding long silica nanotubes after removal of the peptide substrate via calcination [47]. The morphologies of silica nanomaterials can easily be tuned by changing the ratio of peptide to silica precursor, the pH of the solution, and the aging period [62]. Furthermore, more complex interfacial processes are allowed and different morphologies can be obtained just by introducing 3-aminopropyl triethoxysilane (APTES) as a part of the precursor [63]. Through careful control of the ratio of APTES and TEOS, and their feeding order, various “string of beads” silica morphologies or nanofibers can be generated [63]. These results not only improve our understanding of peptide-template- directed synthesis of biological silica formation, but also bring SLPs closer to practical applications.

We have also demonstrated a new and easy route to produce 1D Pt nanostructures with controllable morphologies through the combination of Ac-I_3K-NH_2 with P7A peptide (TLHVSSY) [64]. The Ac-I_3K-NH_2 nanotubes function as a template and P7A serves as a capping agent to achieve switching between ordered and discrete 1D Pt nanoparticle (NP) superstructures. The synthesis strategy of the 1D Pt nanostructures is schematically shown in Figure 7. The continuous and ordered 1D Pt morphology has a significantly improved electrochemical performance for hydrogen and methanol electro-oxidation in comparison with either 1D discrete Pt nanoparticle assemblies or isolated Pt nanoparticles [64].

3.3 Antibacterial and antitumor agents

Most natural and synthetic antimicrobial peptides are cationic and amphiphilic [79]. These structural features enable the peptides to interact well with bacterial and cancer cell membranes that are negatively charged, which eventually leads to membrane damage and cell death. The membranes in animal cells tend to have no net charge, however, and are

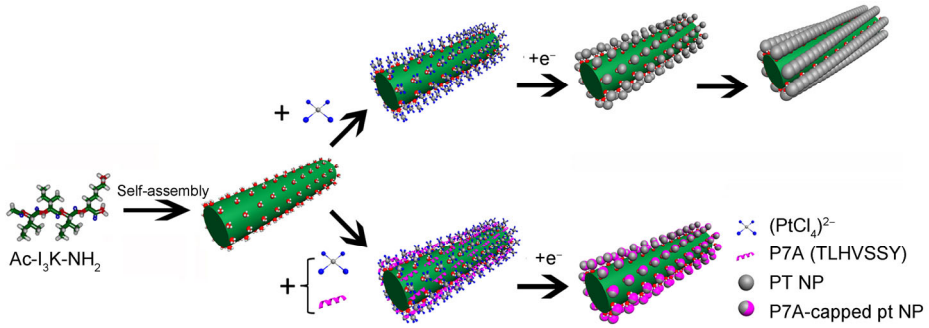

Figure 7 Schematic synthesis strategy of 1D Pt nanostructures. The first step is Ac-I_3K-NH_2 self-assembly, which leads to nanofibril formation (green column). The second step is anchoring Pt NPs on the peptide nanofibril surface in the presence or absence of P7A, which leads to the formation of a well-ordered array or a discrete distribution of the Pt nanostructures. P7A, a peptide-capping agent, clearly alters the morphological patterns of the Pt nanostructures on the template surface [64].

therefore unaffected by cationic peptides. The effectiveness of antimicrobial activities of antimicrobial peptides can be achieved by tuning their cationic charges and hydrophobicity [80]. Ac-A_mK-NH_2 (m = 3, 6, 9) peptides exhibit varying extents of antimicrobial and anticancer activity as the length of hydrophobic tail increases [65, 66]. As indicated above, these SLPs display an increasing propensity for aggregation with the number of hydrophobic alanine residues; in addition, the size and shape of the aggregates show a steady transition from the loose peptide stacks formed by Ac-A_3K-NH_2 and the long nanofibrils formed by Ac-A_6K-NH_2 to the short and thin nanorods formed by Ac-A_9K-NH_2. In parallel to these morphological changes, the antimicrobial capacity and the antitumor activity of the SLPs show a positive correlation with the increase of self-assembling propensity. Ac-A_9K-NH_2 exhibited the best killing capacity against Gram-negative and Gram-positive bacteria as well as various tumor cells. These peptides, like natural antibacterial peptides, killed bacteria and tumor cells via the permeation of cell membranes (Figure 8) [65, 67]. Because these CAPs mainly act on the target cell membranes via a non-receptor-mediated pathway, it is more difficult for bacteria and cancer cells to develop resistance to them than to conventional chemotherapeutic agents. Furthermore, the short peptide is stable in serum and does not induce the non-immunological effect of lymphocytes [67]. Low toxicity to normal mammalian cells, weak immunogenic responses, and high structural stability against degradation would also make this short peptide highly attractive as an antibacterial and antitumor agent.

4 Perspectives

Although synthetic peptides are currently expensive for widespread use, the short length of SLPs, together with tremendous progresses in synthetic methodologies and recombinant production in recent years, makes their large-scale production at low cost feasible in the near future.

The inherent amphiphilicity of SLPs, in combination with hydrogen boding between peptide backbones, easily drives them to self-assemble in water into various nanostructures. Studies are showing that the cooperative action of hydrogen bonding, hydrophobic interaction, and electrostatic repulsion dictate the final self-assembled nanostructures of SLPs. Given the well-understood principles governing the self-assembly of SLPs, the diverse properties (e.g. hydrophobicity, aromaticity, geometry, charge and isoelectric point) of various amino acids and their propensities for forming different secondary structures, as well as the short length and structural simplicity of SLPs, make it feasible to mediate not only their properties but also self-assembled nanostructures at the molecular level by carefully engineering their amino-acid sequences.

Upon self-assembly in water, the charged residues are distributed on the surface of the assembled nanostructures. This feature not only endows the assemblies with biological and chemical functionality but also makes them biologically and chemically modifiable and sensitive to environmental stimuli (e.g., pH, ionic strength, metal ions, and enzymes). By taking advantage of the positive charge of lysine and its catalytic ability for silicification, we have demonstrated applications of the self-assemblies of lysine-containing SLPs (Ac-A_9K-NH_2 and Ac-I_3K-NH_2) as antibacterial agents and templates for the biomimetic synthesis of silica nanomaterials. Histidine (H) can bind transition-metal ions such as Zn^{2+} and Cu^{2+}; Castelletto *et al.* [81] used this mechanism to tune the self-assembly of A_6H by the addition of Zn^{2+}. Very recently, they designed A_6RGD by using bioactive-motif RGD as the head group and found that A_6RGD films promote the attachment of human cornea stromal fibroblasts (hCSFs) [82]. We must also note that, charged residues are substrates that many enzymes can work on, which means that the properties or functionalities of SLP- based materials can be enzymatically controlled. For example, lysine oxidase or plasma amine oxidase can oxidize the primary amine of lysine to aldehyde. Because the aldehyde formed can spontaneously react with another amine to form a Schiff base or undergo an aldol condensation with another aldehyde,

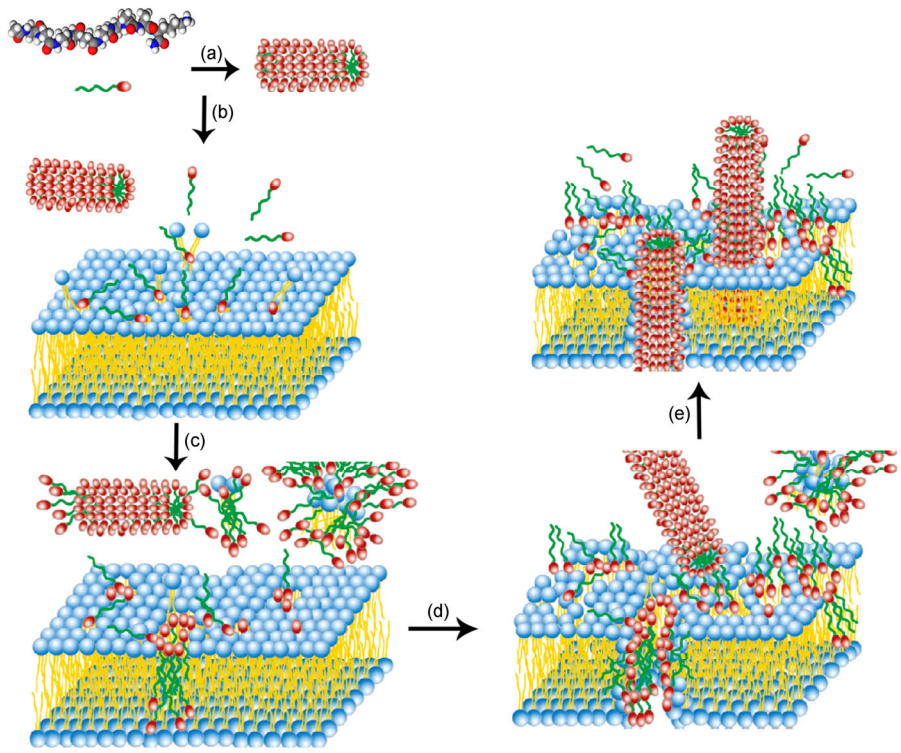

Figure 8 A schematic illustration of mechanisms of action adopted by A_9K for bacterial membrane permeation and disruption. The red rods represent A_9K nanorods. (a) The A_9K molecules assemble into nanorods with the positive charges outside; (b) the monomers may also flip over and insert into the outer membrane surface; (c) they can then insert into the inner leaf of the membrane, forming a through barrel or micelle to cause leakage or lysis; (d, e) the nanorods may also attack the cell membrane through electrostatic attraction or local hydrophobic affinity, in this process they would lift some lipids out of the membrane and make the membrane unstable, thus causing the nanorods to flip into the membrane bilayer [65].

the mechanical strength of peptide gels containing lysine has been increased by using the two enzymes [83, 84].

Provided that the cost bottleneck can be overcome, the improved understanding of SLP self-assembly principles and the incorporation of new functional and responsive elements can be expected to bring to more functional self-assembling SLP building blocks and more exciting potential applications in the coming decades. In addition, some other applications will be realized in the near future.

5 Conclusions

Peptide self-assembly provides a powerful bottom-up approach to the fabrication of materials with well-defined nanostructures and unique functions. Relative to other self-assembling peptides, SLPs consist exclusively of amino acids; their length is short (typically <10 residues); and their structure, which is rather simple, is similar to conventional surfactants. These structural features make them extremely attractive for studies of the principles of peptide self-assembly and practical applications. Herein we reported recent advances in their self-assembly principles and applications. The reported findings not only reveal the roles of various noncovalent forces and their interplay in the self-assembly of SLPs but also demonstrate their potential for diverse applications, from membrane protein stabilization and antimicrobial/anticancer agents to nanofabrication and biomineralization. Future challenges or studies will focus more on large-scale production, design of new functional SLPs with targeted properties, and exploiting new and improved applications.

This work was supported by the National Natural Science Foundation of China (21373270, 21033005) and the Natural Science Foundation of Shandong Province (JQ201105). Xu H. acknowledges the support of the Program for New Century Excellent Talents in University (NCET-11-0735).

1 Whitesides GM, Grzybowski B. Self-assembly at all scales. *Science*, 2002, 295: 2418–2421
2 Whitesides GM, Boncheva M. Beyond molecules: self-assembly of mesoscopic and macroscopic components. *Proc Natl Acad Sci USA*, 2002, 99: 4769–4774
3 Dobson CM. Protein folding and misfolding. *Nature*, 2003, 426: 884–890
4 Winfree E, Liu F, Wenzler LA, Seeman NC. Design and self-assembly of two-dimensional DNA crystals. *Nature*, 1998, 394: 539–544
5 Rothemund PWK. Folding DNA to create nanoscale shapes and patterns. *Nature*, 2006, 440: 297–302
6 Ghadiri MR, Granja JR, Milligan RA, McRee DE, Khazanovich N. Self-assembling organic nanotubes based on a cyclic peptide archi-

tecture. *Nature*, 1993, 366: 324–347
7 Zhang S, Holmes T, Lockshin C, Rich A. Spontaneous assembly of a self-complementary oligopeptide to form a stable macroscopic membrane. *Proc Natl Acad Sci USA*, 1993, 90: 3334–3338
8 Hartgerink JD, Beniash E, Stupp SI. Self-assembly and mineralization of peptide-amphiphile nanofibers. *Science*, 2001, 294: 1684–1688
9 Reches M, Gazit E. Casting metal nanowires within discrete self-assembled peptide nanotubes. *Science*, 2003, 300: 625–627
10 Zhang S. Fabrication of novel biomaterials through molecular self-assembly. *Nat Biotech*, 2003, 21: 1171–1178
11 Schnur JM. Lipid tubules: a paradigm for molecularly engineered structures. *Science*, 1993, 262: 1669–1676
12 Gazit E. Self-assembled peptide nanostructures: the design of molecular building blocks and their technological utilization. *Chem Soc Rev*, 2007, 36: 1263–1269
13 Zhao X, Zhang S. Molecular designer self-assembling peptides. *Chem Soc Rev*, 2006, 35: 1105–1110
14 Ulijn RV, Smith AM. Designing peptide based nanomaterials. *Chem Soc Rev*, 2008, 37: 664–675
15 Zhao X, Pan F, Xu H, Yaseen M, Shan H, Hauser CAE, Zhang S, Lu JR. Molecular self-assembly and applications of designer peptide amphiphiles. *Chem Soc Rev*, 2010, 39: 3480–3498
16 Cui H, Webber MJ, Stupp SI. Self-assembly of peptide amphiphiles: from molecules to nanostructures to biomaterials. *Biopolymers*, 2010, 94: 1–18
17 Yan X, Zhu P, Li J. Self-assembly and application of diphenylalanine-based nanostructures. *Chem Soc Rev*, 2010, 39: 1877–1890
18 Hamley IW. Self-assembly of amphiphilic peptides. *Soft Matter*, 2011, 7: 4122–4138
19 Loo Y, Zhang S, Hauser CAE. From short peptides to nanofibers to macromolecular assemblies in biomedicine. *Biotechnol Adv*, 2012, 30: 593–603
20 Hosseinkhani H, Hong PD, Yu DS. Self-assembled proteins and peptides for regenerative medicine. *Chem Rev*, 2013, 113: 4837–4861
21 Fichman G, Gazit E. Self-assembly of short peptides to form hydrogels: design of building blocks, physical properties and technological applications. *Acta Biomater*, 2014, 10: 1671–1682
22 Ghadiri MR, Granja JR, Buehler LK. Artificial transmembrane ion channels from self-assembling peptide nanotubes. *Nature*, 1994, 369: 301–304
23 Fernandez-Lopez S, Kim HS, Choi EC, Delgado M, Granja JR, Khasanov A, Kraehenbuehl K, Long G, Weinberger DA, Wilcoxen KM, Ghadiri MR. Antibacterial agents based on the cyclic D,L-α-peptide architecture. *Nature*, 2001, 412: 452–455
24 Kisiday J, Jin M, Kurz B, Hung H, Semino C, Zhang S, Grodzinsky AJ. Self-assembling peptide hydrogel fosters chondrocyte extracellular matrix production and cell division: implications for cartilage tissue repair. *Proc Natl Acad Sci USA*, 2002, 99: 9996–10001
25 Holmes TC, de Lacalle S, Su X, Liu G, Rich A, Zhang S. Extensive neurite outgrowth and active synapse formation on self-assembling peptide scaffolds. *Proc Natl Acad Sci USA*, 2000, 97: 6728–6733
26 Koutsopoulos S, Unsworth LD, Nagai Y, Zhang S. Controlled release of functional proteins through designer self-assembling peptide nanofiber hydrogel scaffold. *Proc Natl Acad Sci USA*, 2009, 106: 4623–4628
27 Aggeli A, Bell M, Boden N, Keen JN, Knowles PF, McLeish TCB, Pitkeathly M, Radford SE. Responsive gels formed by the spontaneous self-assembly of peptides into polymeric β-sheet tapes. *Nature*, 1997, 386: 259–262
28 Collier JH, Messersmith PB. Enzymatic modification of self-assembled structures with tissue transglutaminase. *Bioconjugate Chem*, 2003, 14: 748–755
29 Hartgerink JD, Beniash E, Stupp SI. Peptide-amphiphile nanofibers: a versatile scaffold for the preparation of self-assembling materials. *Proc Natl Acad Sci USA*, 2002, 99: 5133–5138
30 Cui H, Muraoka T, Cheetham AG, Stupp SI. Self-assembly of giant peptide nanobelts. *Nano Lett*, 2009, 9: 945–952
31 Zhang S, Greenfield MA, Mata A, Palmer LC, Bitton R, Mantei JR, Aparicio C, de la Cruz MO, Stupp SI. A self-assembly pathway to aligned monodomain gels. *Nat Mater*, 2010, 9: 594–601
32 Makovitzki A, Baram J, Shai Y. Antimicrobial lipopolypeptides composed of palmitoyl di- and tricationic peptides: *in vitro* and *in vivo* activities, self-assembly to nanostructures, and a plausible mode of action. *Biochemistry*, 2008, 47: 10630–10636
33 Schneider JP, Pochan DJ, Ozbas B, Rajagopal K, Pakstis L, Kretsinger J. Responsive hydrogels from the intramolecular folding and self-assembly of a designed peptide. *J Am Chem Soc*, 2002, 124: 15030–15037
34 Haines-Butterick L, Rajagopal K, Branco M, Salick D, Rughani R, Pilarz M, Lamm MS, Pochan DJ, Schneider JP. Controlling hydrogelation kinetics by peptide design for three-dimensional encapsulation and injectable delivery of cells. *Proc Natl Acad Sci USA*, 2007, 104: 7791–7796
35 Smith AM, Williams RJ, Tang C, Coppo P, Collins RF, Turner ML, Saiani A, Ulijn RV. Fmoc-diphenylalanine self assembles to a hydrogel via a novel architecture based on π-π interlocked β-sheets. *Adv Mater*, 2008, 20: 37–41
36 Lu K, Jacob J, Thiyagarajan P, Conticello VP, Lynn DG. Exploiting amyloid fibril lamination for nanotube self-assembly. *J Am Chem Soc*, 2003, 125: 6391–6393
37 Tao K, Wang J, Zhou P, Wang C, Xu H, Zhao X, Lu JR. Self-assembly of short Aβ (16–22) peptides: effect of terminal capping and the role of electrostatic interaction. *Langmuir*, 2011, 27: 2723–2730
38 Dong H, Paramonov SE, Aulisa L, Bakota EL, Hartgerink JD. Self-assembly of multidomain peptides: balancing molecular frustration controls conformation and nanostructures. *J Am Chem Soc*, 2007, 129: 12468–12472
39 Bakota E, Wang Y, Danesh FR, Hartgerink JD. Injectable multidomain peptide nanofiber hydrogel as a delivery agent for stem cell secretome. *Biomacromolecules*, 2011, 12: 1651–1657
40 Banwell EF, Abelardo ES, Adams DJ, Birchall MA, Corrigan A, Donald AM, Kirkland M, Serpell LC, Butler MF, Woolfson DN. Rational design and application of responsive α-helical peptide hydrogels. *Nat Mater*, 2009, 8: 596–600
41 Vauthey S, Santoso S, Gong H, Watson N, Zhang S. Molecular self-assembly of surfactant-like peptides to form nanotubes and nanovesicles. *Proc Natl Acad Sci USA*, 2002, 99: 5355–5360
42 Santoso S, Hwang W, Hartman H, Zhang S. Self-assembly of surfactant-like peptides with variable glycine tails to form nanotubes and nanovesicles. *Nano Lett*, 2002, 2: 687–691
43 von Maltzahn G, Vauthey S, Santoso S, Zhang S. Positively charged surfactant-like peptides self-assembly into nanostructures. *Langmuir*, 2003, 19: 4332–4337
44 Kiley P, Zhao X, Vaughn M, Baldo MA, Bruce BD, Zhang S. Self-assembling peptide detergents stabilize isolated photosystem I on a dry surface for an extended time. *PLoS Biol*, 2005, 3: e230
45 Koutsopoulos S, Kaiser L, Maria H, Eriksson M, Zhang S. Designer peptide surfactants stabilize diverse functional membrane proteins. *Chem Soc Rev*, 2012, 41: 1721–1728
46 Mishra A, Loo Y, Deng R, Chuah Y J, Hee HT, Ying JY, Hauser CAE. Ultrasmall natural peptides self-assemble to strong temperature-resistant helical fibers in scaffolds suitable for tissue engineering. *Nano Today*, 2011, 6: 232–239
47 Xu H, Wang Y, Ge X, Han S, Wang S, Zhou P, Shan H, Zhao X, Lu JR. Twisted nanotubes formed from ultrashort amphiphilic peptide I_3K and their templating for the fabrication of silica nanotubes. *Chem Mater*, 2010, 22: 5165–5173
48 Bucak S, Cenker C, Nasir I, Olsson U, Zackrisson M. Peptide nanotube nematic phase. *Langmuir*, 2009, 25: 4262–4265
49 Nagai A, Nagai Y, Qu H, Zhang S. Dynamic behaviors of lipid-like self-assembling peptide A_6D and A_6K nanotubes. *J Nanosci Nanotech*, 2007, 7: 1–7
50 Yang SJ, Zhang S. Self-assembling behavior of designer lipid-like peptides. *Supramol Chem*, 2006, 18: 389–396
51 van Hell AJ, Costa CICA, Flesch FM, Sutter M, Jiskoot W, Crommelin DJA, Hennink WE, Mastrobattista E. Self-assembly of recom-

binant amphiphilic oligopeptides into vesicles. *Biomacromolecules*, 2007, 8: 2753–2761
52 Khoe U, Yang Y, Zhang S. Self-assembly of nanodonut structure from a cone-shaped designer lipid-like peptide surfactant. *Langmuir*, 2009, 25: 4111–4114
53 Wang J, Han S, Meng G, Xu H, Xia D, Zhao X, Schweins R, Lu JR. Dynamic self-assembly of surfactant-like peptides A_6K and A_9K. *Soft Matter*, 2009, 5: 3870–3878
54 Han S, Cao S, Wang Y, Wang J, Xia D, Xu H, Zhao X, Lu JR. Self-assembly of short peptide amphiphiles: the cooperative effect of hydrophobic interaction and hydrogen bonding. *Chem Eur J*, 2011, 17: 13095–13102
55 Han S, Xu W, Cao M, Wang J, Xia D, Xu H, Zhao X, Lu JR. Interfacial adsorption of cationic peptide amphiphiles: a combined study of *in situ* spectroscopic ellipsometry and liquid AFM. *Soft Matter*, 2012, 8: 645–653
56 Baumann MK, Textor M, Reimhult E. Understanding self-assembled amphiphilic peptide supramolecular structures form primary structure helix propensity. *Langmuir*, 2008, 24: 7645–7647
57 Hauser CAE, Deng R, Mishra A, Loo Y, Khoe U, Zhuang F, Cheong DW, Accardo A, Sullivan MB, Riekel C, Ying JY, Hauser UA. Natural tri- to hexapeptides self-assemble in water to amyloid β-type fiber aggregates by unexpected α-helical intermediate structures. *Proc Natl Acad Sci USA*, 2011, 108: 1361–1366
58 Xu H, Wang J, Han S, Wang J, Yu D, Zhang H, Xia D, Zhao X, Waigh TA, Lu JR. Hydrophobic-region-induced transitions in self-assembled peptide nanostructures. *Langmuir*, 2009, 25: 4115–4123
59 Khoe U, Yang Y, Zhang S. Synergetic effect and hierarchical nanostructure formation in mixing two designer lipid-like peptide surfactants Ac-A_6D-OH and Ac-A_6K-NH_2. *Macromol Bio Sci*, 2008, 8: 1060–1067
60 Zhao Y, Wang J, Deng L, Zhou P, Wang S, Wang Y, Xu H, Lu JR. Tuning the self-assembly of short peptides via sequence variations. *Langmuir*, 2013, 29: 13457–13464
61 Ge B, Yang F, Yu D, Liu S, Xu H. Designer amphiphilic short peptides enhance thermal stability of isolated photosystem-I. *PLoS One*, 2010, 5: e10233
62 Wang S, Ge X, Xue J, Fan H, Mu L, Li Y, Xu H, Lu JR. Mechanistic processes underlying biomimetic synthesis of silica nanotubes from self-assembled ultrashort peptide templates. *Chem Mater*, 2011, 23: 2466–2474
63 Wang S, Xue J, Ge X, Fan H, Xu H, Lu JR. Biomimetic synthesis of silica nanostructures with controllable morphologies and sizes through interfacial interactions. *Chem Commun*, 2012, 48: 9415–9417
64 Tao K, Wang J, Li Y, Xia D, Shan H, Xu H, Lu JR. Short peptide-directed synthesis of one-dimensional platinum nanostructures with controllable morphologies. *Sci Rep*, 2013, 3: 2565
65 Chen C, Pan F, Zhang S, Hu J, Cao M, Wang J, Xu H, Zhao X, Lu JR. Antibacterial activities of short designer peptides: a link between propensity for nanostructuring and capacity for membrane destabilization. *Biomacromolecules*, 2010, 11: 402–411
66 Chen C, Hu J, Zhang S, Zhou P, Zhao X, Xu H, Zhao X, Yaseen M, Lu JR. Molecular mechanism of antibacterial and antitumor actions of designer surfactant-like peptides. *Biomaterials*, 2012, 33: 592–603
67 Xu H, Chen C, Hu J, Zhou P, Zeng P, Cao C, Lu JR. Dual modes of antitumor action of an amphiphilic peptide A_9K. *Biomaterials*, 2013, 34: 2731–2737
68 Hamley IW, Dehsorkhi A, Castellotto V. Self-assembled arginine-coated peptide nanosheets in water. *Chem Commn*, 2013, 49: 1850–1852
69 Dehsorkhi A, Castelletto V, Hamley IW. Interaction between a cationic surfactant-like peptide and lipid vesicles and its relationship to antimicrobial activity. *Langmuir*, 2013, 29: 14246–14253
70 Huang R, Qi W, Su R, Zhao J, He Z. Solvent and surface controlled self-assembly of diphenylalanine peptide: from microtubes to nanofibers. *Soft Matter*, 2011, 7: 6418–6421
71 Nagarajan R, Ruckenstein E. Theory of surfactant self-assembly: a predictive molecular thermodynamic approach. *Langmuir*, 1991, 7: 2934–2969
72 Daniel L, Minor J, Kim PS. Measurement of the β-sheet-forming propensities of amino acids. *Nature*, 1994, 367: 660–663
73 Nagarajan R. Molecular packing parameters and surfactant self-assembly: the neglected role of the surfactant tail. *Langmuir*, 2002, 18: 31–38
74 Cao M, Wang Y, Ge X, Cao C, Wang J, Xu H, Xia D, Zhao X, Lu JR. Effects of anions on nanostructuring of cationic amphiphilic peptides. *J Phys Chem B*, 2011, 115: 11862–11871
75 Zhao X, Nagai Y, Reeves PJ, Kiley P, Khorana HG, Zhang S. Designer short peptide surfactants stabilize G protein-coupled receptor bovine rhodopsin. *Proc Natl Acad Sci USA*, 2006, 103: 17707–17712
76 Wallin E, Heijne GV. Genome-wide analysis of integral membrane proteins from eubacterial, archaean, and eukaryotic organisms. *Protein Sci*, 1998, 7: 1029–1038
77 Loll PJ. Membrane protein structural biology: the high throughput challenge. *J Struct Biol*, 2003, 142: 144–153
78 Nilsson J, Persson B, von Heijne G. Comparative analysis of amino acid distributions in integral membrane proteins from 107 genomes. *Proteins*, 2005, 60: 606–616
79 Zasloff M. Antimicrobial peptides of multicellular organisms. *Nature*, 2002, 415: 389–395
80 Dathe M, Wieprecht T. Structural features of helical antimicrobial peptides: their potential to modulate activity on model membranes and biological cells. *BBA-Biomembranes*, 1999, 1462: 71–87
81 Castelletto V, Hamley IW, Segarra-Maset MD, Gumbau CB, Miravet JF, Escuder B, Seitsonen J, Ruokolainen J. Tuning chelation by the surfactant-like peptide A_6H using predetermined pH values. *Biomacromolecules*, 2014, 15: 591–598
82 Castelletto V, Gouveia RM, Connon CJ, Hamley IW, Seitsonen J, Nykänen A, Ruokolainen J. Alanine-rich amphiphilic peptide containing the RGD cell adhesion motif: a coating material for human fibroblast attachment and culture. *Biomater Sci*, 2014, 2: 362–369
83 Bakota EL, Aulisa L, Galler KM, Hartgerink JD. Enzymatic cross-linking of a nanofibrous peptide hydrogel. *Biomacromolecules*, 2011, 12: 82–87
84 Teixeira LSM, Feijen J, van Blitterswijk CA, Dijkstra PJ, Karperien M. Enzyme-catalyzed crosslinkable hydrogels: emerging strategies for tissue engineering. *Biomaterials*, 2012, 33: 1281–1290